

# Characterization of *Arabidopsis thaliana* SMC1 and SMC3: evidence that AtSMC3 may function beyond chromosome cohesion

Wing See Lam\*, Xiaohui Yang\* and Christopher A. Makaroff<sup>‡</sup>

The Department of Chemistry and Biochemistry, Miami University, Oxford, OH 45056, USA

\*These authors contributed equally to this work

<sup>‡</sup>Author for correspondence (e-mail: makaroca@muohio.edu)

Accepted 18 April 2005

Journal of Cell Science 118, 3037-3048 Published by The Company of Biologists 2005

doi:10.1242/jcs.02443

## Summary

Structural maintenance of chromosome (SMC) proteins are conserved in most prokaryotes and all eukaryotes examined. SMC proteins participate in many different aspects of chromosome folding and dynamics. They play essential roles in complexes that are responsible for sister chromatid cohesion, chromosome condensation and DNA repair. As part of studies to better understand SMC proteins and sister chromatid cohesion in plants we have characterized *Arabidopsis* SMC1 and SMC3. Although transcripts for *AtSMC1* and *AtSMC3* are present throughout the plant, transcript levels for the two genes vary between different tissues. Cell fractionation and immunolocalization results showed that AtSMC3 was present in the nucleus and cytoplasm. In the nucleus, it is

primarily associated with the nuclear matrix during interphase and with chromatin from prophase through anaphase in both somatic and meiotic cells. During mitosis and meiosis the protein also co-localized with the spindle from metaphase to telophase. The distribution of AtSMC3 in *syn1* mutant plants indicated that SYN1 is required for the proper binding of *AtSMC3* to meiotic chromosomes, but not the spindle. Data presented here represent the first detailed cytological study of a plant SMC protein and suggest that SMC3 may have multiple functions in plants.

Key words: cohesin complex, chromosome cohesion, mitosis, meiosis, *Arabidopsis thaliana*

## Introduction

Structural maintenance of chromosome (SMC) proteins play critical roles in chromosome dynamics from bacteria to vertebrates (Cobbe and Heck, 2000; Gruber et al., 2003; Hirano, 2002; Jessberger, 2002). Members of the SMC family of proteins share five conserved structural domains, including an N-terminal NTP-binding motif, a C-terminal DA box and two central coiled-coil domains separated by a hinge domain. The head and tail of SMC proteins can fold back on themselves to form an ABC-like ATP-binding cassette (Haering et al., 2002). Bacteria encode one SMC protein, which functions as a homodimer, whereas eukaryotes have multiple SMC proteins that form heterodimers, which are connected at the hinge domains (Haering et al., 2002; Hirano, 2002; Soppa, 2001).

Eukaryotic SMC proteins can be divided into three classes based on their function. (1) The condensins, SMC2 and SMC4, regulate chromosome condensation and organize long linear chromosomes into compact structures during cell division (Hagstrom et al., 2002; Ono et al., 2003; Schmiesing et al., 2000). (2) Cohesin complexes, which contain SMC1 and SMC3, are responsible for maintaining sister chromatid cohesion after DNA replication and help facilitate the proper segregation of chromosomes (Haering et al., 2002; Klein, 1999; Michaelis et al., 1997; Yokobayashi et al., 2003). (3) DNA recombination and repair complexes contain SMC5 and SMC6 and participate in postreplicative and recombinational

repair of DNA lesions and double-strand breaks (Fousteri and Lehmann, 2000; Taylor et al., 2001). SMC heterodimers associate with different sets of non-SMC subunits to assemble fully functional SMC holocomplexes (Cobbe and Heck, 2000; Hirano, 2002).

SMC1 and SMC3 are two of the most extensively studied SMC proteins. Along with the two non-SMC subunits SCC1/REC8 and SCC3 (SA) they form the cohesin complex. Mutations in SMC cohesin proteins cause premature sister-chromatid separation and the mis-segregation of chromosomes (Losada et al., 1998; Michaelis et al., 1997; Strunnikov et al., 1993).

In *Saccharomyces cerevisiae* the mitotic cohesin complex first associates with chromosomes during late G1 of the mitotic cell cycle and establishes sister-chromatid cohesion in S phase (Uhlmann and Nasmyth, 1998). At the metaphase to anaphase transition Scc1 is cleaved by separase (Esp1), which facilitates the release of cohesion and sister chromatid separation (Uhlmann et al., 1999; Uhlmann et al., 2000). It is thought that following Scc1 cleavage, Scc1 and Scc3 dissociate from DNA, whereas Smc1 and Smc3 remain bound through anaphase (Tanaka et al., 1999).

The animal mitotic cohesin complex consists of SMC1 $\alpha$ , SMC3, SCC1 and either SA1 or SA2 (stromal antigen protein) (Losada et al., 2000). The distribution of animal cohesin proteins is also cell cycle dependent but different from that

observed in yeast. The vertebrate cohesin complex first associates with chromosomal DNA during interphase, with the majority of cohesin dissociating from chromosome arms and moving to the cytoplasm prior to mitosis (Sumara et al., 2002; Waizenegger et al., 2000). This early release of cohesin is thought to allow the tightly associated chromatids to condense during prophase (Losada et al., 2002). Similar to the situation in yeast, cleavage of SCC1 by separase at the metaphase-anaphase transition, results in sister chromatid separation (Hauf et al., 2001).

Cohesin complexes play a similar role in chromosome segregation during meiosis. The yeast meiotic cohesin complex consists of Smc1, Smc3, Scc3 and Rec8, the meiotic paralog of Scc1 (Klein, 1999; Lin et al., 1992). During meiosis the release of cohesin, which appears to be established during premeiotic S phase, is resolved in two steps (Buonomo et al., 2000). At the onset of anaphase I, cohesin is released from the chromosome arms in an Esp1-dependent process to allow homologous chromosome disjunction. It persists at the centromeres until anaphase II when it is released to allow the segregation of sister chromatids.

A similar situation exists for the mammalian meiotic cohesin complex, which consists of SMC1 $\beta$ , SMC3, REC8 and STAG3 (Prieto, 2001; Revenkova et al., 2001). Although the proteins are known to act as a complex, immunolocalization studies in rat detected the proteins at different times and locations during meiosis (Eijpe et al., 2000; Eijpe et al., 2003). At this time it is not clear if these differences are due to conformational variations that affect antibody binding or if the proteins actually bind chromosomes independently.

Much less is known about the cohesion machinery in plants. In *Arabidopsis thaliana*, SYN1 (DIF1), which is a REC8 ortholog, is essential for chromosome cohesion and homologous chromosome pairing during meiosis (Bai et al., 1999; Bhatt et al., 1999; Cai et al., 2003; Peirson et al., 1997). SYN1 is found along chromosome arms from approximately meiotic interphase I to metaphase I (Cai et al., 2003). In addition to SYN1, *Arabidopsis* contains three additional SCC1 paralogs, SYN2, SYN3 and SYN4, which are expressed throughout the plant, suggesting that they may participate in mitotic cohesion (Dong et al., 2001).

*Arabidopsis* also contains predicted genes for SCC3 (AT2g47980), SMC1, SMC3, SMC4, and two copies of SMC2 (*AtCAP-E1* and *AtCAP-E2*). *Arabidopsis* knockout mutants have been characterized for *AtCAP-E1* (*titan3*, *AtCAP-E1*<sup>-/-</sup>), *AtCAP-E2* (*AtCAP-E2*<sup>-/-</sup>), *SMC1* (*titan8-1* and *titan8-2*) and *SMC3* (*titan7-1* and *titan7-2*) (Liu et al., 2002; Liu and Meinke, 1998; Siddiqui et al., 2003). The *titan3* mutant has enlarged endosperm nuclei and aberrant mitotic figures, but plants appear to develop normally (Liu and Meinke, 1998). An *AtCAP-E2* mutant showed no obvious phenotype; however, embryo lethality was observed for double homozygous *AtCAP-E1*<sup>-/-</sup>, *AtCAP-E2*<sup>-/-</sup> mutants and *AtCAP-E1*<sup>-/-</sup>, *AtCAP-E2*<sup>+/-</sup> plants (Siddiqui et al., 2003). *SMC1* (*ttn8-1*, *ttn8-2*) and *SMC3* (*ttn7-1*, *ttn7-2*) knockout plants show defects in both the embryo and endosperm and arrest early in seed development (Liu et al., 2002). While analysis of plants containing mutations in the SMC genes has provided some insight into their role, a detailed analysis of the distribution and localization of SMC proteins has not been reported in plants. Given the differences in distribution patterns between the yeast and

animal SMC proteins as well as our relative lack of information on plant SMC proteins, the mechanism of how plant SMC cohesin proteins function during cell division is still unclear.

We report here a characterization of *Arabidopsis* SMC1 (AtSMC1) and SMC3 (AtSMC3) designed to better understand the structure and functions of plant SMC proteins. Localization studies show that AtSMC3 is found in both the cytoplasm and nucleus of somatic and generative cells. In the nucleus the protein is present on the chromosomes and in the nuclear matrix. During mitosis and meiosis AtSMC3 localizes with the sister chromatids from prophase until late anaphase. Interestingly, beginning at metaphase and extending through telophase it is also associated with the spindle. These results indicate that in addition to its conserved role in sister chromatid cohesion, AtSMC3 may have additional roles in plant cells.

## Materials and Methods

### Plant material

Seeds of wild-type *Arabidopsis thaliana*, ecotypes Landsberg *erecta*, Wassilewskija (WS), Columbia and *syn1*, were grown on a commercial potting mix in a growth chamber at 22°C with a 16:8 hour light:dark cycle. *syn1* has been described previously (Bai et al., 1999). Approximately 3 weeks after germination, 0.3–0.7 mm buds were collected from prebolting plants, fixed and analyzed as described below.

*Arabidopsis* suspension cells (ecotype Landsberg *erecta*), generously provided by Jonathon Jones, were cultured in cell medium [3.2 g/l Gamborg's B-5 vitamins, 3% (w/v) sucrose, 0.5 g/l Mes 1.1 mg/l of 2,4-dichlorophenoxyacetic acid (2,4-D), and adjusted to pH 5.7 with KOH] at room temperature with agitation.

### cDNA cloning and expression analysis

Total RNA, isolated from Columbia bud tissue was subjected to oligo(dT)-directed cDNA synthesis. The resulting cDNA population was used as a template in PCR to analyze the *AtSMC1*, *AtSMC3*, *AtSMC1-3'UTR* and *PTPG* transcripts. The position of primers used for the amplification reactions are shown in Fig. 1. The resulting cDNAs were sequenced and analyzed with DNASTar (DNASTar Inc., Madison, WI, USA) and PSORT (Berger et al., 1995).

*AtSMC1*, *AtSMC1-3'UTR*, *AtSMC3* and *PTPG* expression patterns were analyzed using reverse transcription PCR (RT-PCR) and real time PCR. Poly(A)+ RNA (150 ng) from roots, leaves, stems and buds of wild-type plants was subjected to RT-PCR. Primers for *ACTIN8* (*ACT8*) were used as a control to standardize the cDNA (An et al., 1996). PCR products were analyzed in 0.8% agarose gels stained with ethidium bromide followed by Southern blot analysis. Probes were labeled with [<sup>32</sup>P]dCTP and were specific for *AtSMC1*, *AtSMC1-3'UTR*, *AtSMC3*, *PTPG* or *ACT8*. Radioactivity was detected using a Molecular Dynamics Phosphorimager (Sunnyvale, CA, USA).

Poly(A)+ RNA (150 ng) from roots, leaves, stems and buds of wild-type plants were also subjected to oligo(dT)-directed cDNA synthesis using an iScript cDNA synthesis kit (Bio-Rad Laboratories). Serial dilutions of the cDNAs and the primers were used to optimize the real-time PCR assay following the manufacturer's instructions. Primers were designed using PrimerExpress version 1.0 (Applied Biosystems). Real-time PCR assays were carried out in an iCycler thermalcycler with iCycle iQ Real-Time PCR Detection System (Bio-Rad Laboratories, Hercules, CA, USA), using the following sequence: 3 minutes at 95°C, 50 cycles of 30 seconds at 95°C and 2 minutes at 60°C, 1 minute at 95°C, 1 minute at 55°C and 80 cycles of 10 seconds at 55°C with an increase of 0.5°C at each cycle. This reaction sequence also provided the assay for the dissociation curves to ensure only one PCR product was generated from each real-time PCR

reaction. Standard curves were constructed for each primer pair to determine their amplification efficiency. The correlation coefficients obtained for *AtSMC1*, *PTPG*, *AtSMC3* and *ACT8* were between 0.995 and 0.962. We were unable to obtain an acceptable correlation coefficient for the *AtSMC1-3'UTR* transcript. Therefore, *AtSMC1-3'UTR* transcript levels could not be analyzed using this technique.

### Antibody production

PCR fragments corresponding to amino acids 1-574 and 1-572 of *AtSMC1* and *AtSMC3*, respectively, were cloned into pET22b and used for over-expression in *E. coli* BL<sub>21</sub>RIL cells. The proteins were purified using nickel-affinity chromatography, followed by SDS-polyacrylamide gel electrophoresis and used for antibody production using standard procedures (Harlow and Lane, 1999). Nonspecific antibodies were removed using acetone powders of *E. coli* protein as described previously (Harlow and Lane, 1999). The anti-*AtSMC3* antibody was specific for *AtSMC3*. It detects a protein corresponding to the N terminus of *AtSMC3*, but not *AtSMC1* (data not shown).

### Cell extraction and western blotting

In situ cell extraction was performed on actively growing *Arabidopsis* suspension cells essentially as described previously (Gregson et al., 2001). The cells were harvested, washed and digested with 1.4% w/v  $\beta$ -glucuronidase and 0.3% w/v pectolyase in 10 mM sodium citrate buffer for 30 minutes at 37°C. After washing with CSK buffer (10 mM Pipes, pH 7.0, 100 mM NaCl, 300 mM sucrose, 3 mM MgCl<sub>2</sub>), the cells were extracted using CSK buffer with 0.5% v/v Triton X-100 for 10 minutes on ice to remove soluble proteins. Cells were then treated with detergent extraction buffer (42.5 mM Tris-HCl, pH 8.3, 8.5 mM NaCl, 2.6 mM MgCl<sub>2</sub>, 1% v/v Tween 20, 0.5% w/v deoxycholic acid) for 10 minutes on ice to remove cytoskeletal proteins. The cells were subsequently treated with CSK buffer with 2 mM CaCl<sub>2</sub> and MgCl<sub>2</sub>, 0.5% v/v Triton X-100 and 100  $\mu$ g/ml DNase I for 30 minutes at 37°C, washed with 0.25 M ammonium sulfate in CSK buffer and fixed with 4% w/v paraformaldehyde. Control cells were treated with the same buffer without DNase I. Between each step cells were centrifuged at 1300 g for a minute, and the supernatant was recovered. The final pellet was washed twice in CSK buffer containing 0.5% v/v Triton X-100 and resuspended in SDS sample buffer.

Total soluble plant tissue extracts were prepared from roots, stems, flower buds, leaves and suspension cells by grinding in liquid nitrogen followed by incubation with isolation buffer [6% w/v SDS, 1% v/v protease inhibitor cocktail (Sigma)] at 60°C for 20 minutes followed by centrifugation at 20,000 g for 5 minutes. Equal amounts (10  $\mu$ g) of total protein or protein from the cell fractionation steps were separated by SDS-PAGE and subjected to western blot analysis with anti-*AtSMC* antibody (1:1000) followed by detection with alkaline phosphatase-conjugated goat anti-rabbit secondary antibody (1:3000) using standard procedures (Harlow and Lane, 1999).

### Immunolocalization

For paraformaldehyde fixation, inflorescences of wild-type plants were fixed for 2 hours at room temperature in buffer A containing 4% paraformaldehyde (Cai et al., 2003). For fixation in methanol:acetone, inflorescences of wild type and the *syn1* mutant were fixed for at least 30 minutes in excess methanol:acetone (4:1, v/v) solution at room temperature, and washed two times with 1× PBS (Eijpe et al., 2000). Anthers were squashed between two perpendicular poly-L-lysine-coated slides. Male meiocytes were dried overnight and covered with a thin layer of agarose/gelatin (0.94% low melting agarose/0.84% gelatin/0.3% w/v sucrose). The meiocytes were then soaked in 1× PBS for 1 hour and treated with 1.4% w/v  $\beta$ -glucuronidase, 0.3% w/v cytohellicase, 0.3% w/v pectolyase, 0.3% w/v cellulase in 10 mM

sodium citrate buffer for 30 minutes at 37°C. After washing in 1× PBS the slides were blocked in blocking buffer (1× PBS, 5% w/v BSA) for 60 minutes and then incubated overnight at 4°C in a moist chamber with rabbit anti-*AtSMC3* antibody (1:500) and mouse anti- $\beta$ -tubulin antibody (1:100; Developmental Studies Hybridoma Bank). The slides were washed eight times (20 minutes each) with 1× PBS and the primary antibody was detected with Alexa Fluor 488-labelled goat anti-rabbit secondary antibody (1:500) with or without Alexa Fluor 594-labelled goat anti-mouse secondary antibody (1:500) overnight at 4°C. After washing, samples were viewed with an Olympus epifluorescent microscope system. Images were captured with a Spot camera system and processed with Adobe Photoshop software (Adobe System, San Jose, CA, USA). All images shown represent examples of the most commonly observed cell at each stage examined. At least 25, but typically 50-100 examples of each cell type were observed.

## Results

### *AtSMC1* and *AtSMC3*

The *Arabidopsis thaliana* genome contains one copy each of *SMC1* (At3g54670) and *SMC3* (At2g27170). As a first step in better understanding the structure and function of the proteins, a series of reverse transcription PCR (RT-PCR) experiments were conducted to isolate full-length cDNAs for the genes (Fig. 1). Sequence analysis of the resulting *AtSMC1* cDNA (accession no. AY567966) indicated it was 3657nt and had the potential to encode a 1218-residue protein with a predicted molecular mass of 141 kDa. The *AtSMC3* cDNA (accession no. AY525642) was 3615 bp long and had the potential to encode a 1204-residue protein with a predicted molecular mass of 139 kDa (Fig. 1). As predicted by the genomic sequences, *AtSMC1* and *AtSMC3* contain all the characteristic features of SMC proteins: an N-terminal ATP-binding domain (*AtSMC1*:AA 1-156; *AtSMC3*:AA1-181), two large coiled-coil regions (*AtSMC1*:AA 157-505 and 671-1041; *AtSMC3*:AA182-500, 672-1012), a hinge region (*AtSMC1*:AA 506-670; *AtSMC3*:AA501-671), and a C-terminal DA box (*AtSMC1*:AA 1042-1218; *AtSMC3*:AA1013-1204).

In animal cells two genes encode *SMC1* proteins, *SMC1 $\alpha$* , which is present in both somatic and meiotic cells and *SMC1 $\beta$* , which is meiosis specific (Revenkova et al., 2001; Revenkova et al., 2004). *SMC1 $\alpha$*  and *SMC1 $\beta$*  are very similar and differ primarily in the presence of a basic C-terminal motif in *SMC1 $\beta$* . Analysis of EST sequences for *AtSMC1* indicated that one of these (RZL46H08F, accession no. AV548094) contained 3'UTR sequences derived from a region 1500 bp downstream of the 3' terminus of the cDNA identified in our studies. Furthermore, a predicted proteophosphoglycan-related (PTPG) gene (At3g54680) is located between *AtSMC1* and the 3'UTR found in RZL46H08F (Fig. 1). This raised the possibility that multiple forms of *AtSMC1* may also be present in *Arabidopsis*.

A series of PCR experiments on oligo(dT)-generated cDNA from flower buds was conducted to examine the relationship between the *AtSMC1* and the predicted *PTPG* gene and determine if multiple forms of *AtSMC1* are produced in *Arabidopsis*. When an *AtSMC1* gene-specific primer (487-Smc1) was used in PCR with an oligo(dT) adaptor primer, two fragments were obtained: an 865 nucleotide (nt) fragment corresponding to *AtSMC1*, and a 978 nt fragment corresponding to the RZL46H08F transcript (referred to as

*AtSMC1-3'UTR*, Fig. 1). Fragments containing the *PTPG* gene were not obtained, indicating that *PTPG* sequences are not part of the *SMC1* transcript. Amplification of fragments containing *PTPG* coding and 3'UTR sequences were, however obtained in PCR with *PTPG*/adapter-primer combinations (*PTPG*, Fig. 1). We therefore concluded that *AtSMC1-3'UTR* and *PTPG* represent two separate transcripts.

Additional RT-PCR experiments using multiple combinations of *AtSMC1* primers throughout the gene did not identify additional alternatively spliced forms of the *AtSMC1* transcript. Given that the *AtSMC1* and *AtSMC1-3'UTR* transcripts differ only in their 3'UTRs, and encode identical proteins, we conclude that *Arabidopsis* only encodes one form of *SMC1* protein.

### *AtSMC1* and *AtSMC3* exhibit different transcript patterns

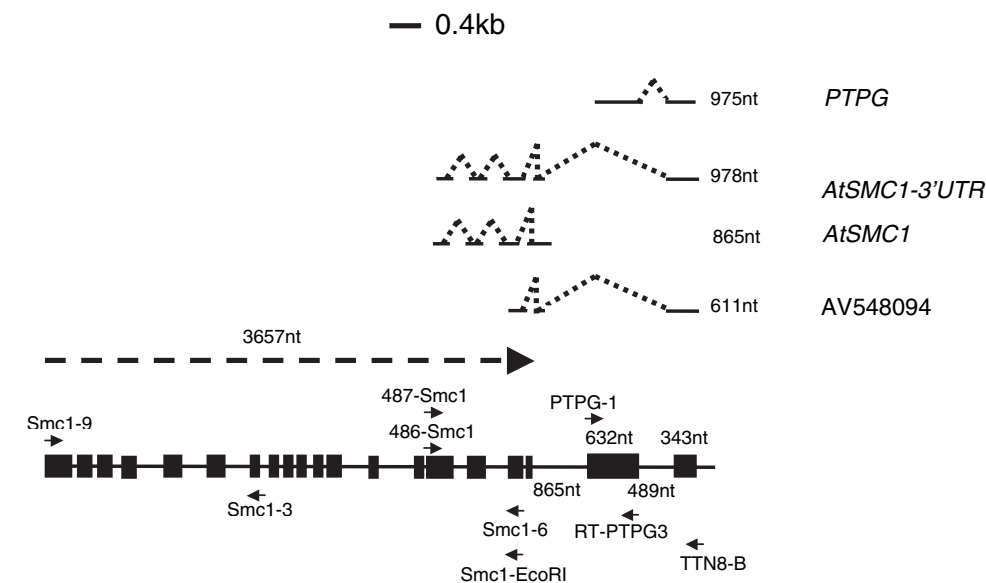
Transcript levels for *AtSMC3*, *PTPG* and the two forms of *AtSMC1* in roots, stems, leaves and flower buds were initially examined using RT-PCR. *ACTIN8* (*ACT8*) was used to standardize the total cDNA used in each reaction (An et al., 1996). Transcripts for *ACT8* and *AtSMC1* were relatively abundant in all tissue samples; 16 cycles were needed to obtain a PCR product (Fig. 2A). In contrast, the *PTPG* and *AtSMC1-3'UTR* transcripts were present at low levels with 30 and 34 cycles, respectively, being required for detection in Southern

blots. *AtSMC3* transcript levels were in general lower than those of *AtSMC1* and were visible in Southern blots after 25 cycles. Interestingly, the genes also showed tissue-specific transcript differences. *AtSMC1* transcripts were highest in bud tissue, with lower levels in stem, leaf and root tissues (Fig. 2A). *AtSMC3* transcripts were highest in buds, followed by leaves, roots and stems (Fig. 2A). The transcript patterns for *PTPG* and *AtSMC1-3'UTR* were similar to *AtSMC3* in that they were highest in buds, followed by leaves, roots and stems.

When the *AtSMC1* and *AtSMC3* transcript differences were further evaluated by real-time PCR we found the same general trend as was observed in the RT-PCR experiments (Fig. 2B). *AtSMC1* and *AtSMC3* transcripts were highest in and approximately equal in buds. In contrast, *AtSMC1* transcripts were approximately 20 times higher in stem RNA than those of *AtSMC3*, while leaf RNA contained approximately ten times more *AtSMC3* RNA than *AtSMC1* RNA. Transcript levels for *AtSMC1* and *AtSMC3* were low and approximately equal in root RNA samples. Transcript levels for *PTPG* were generally low in all tissues.

Therefore, differences in both the overall level and distribution of *AtSMC1* and *AtSMC3* transcripts were observed in different tissues. These results suggest that either the two genes are regulated at a post-transcriptional level or that the two proteins differ in their overall levels.

### *AtSMC1*



### *AtSMC3*

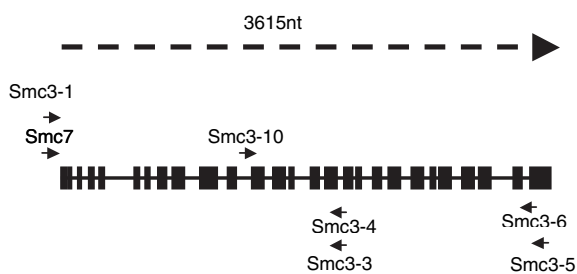


**Fig. 1.** Schematic representation of the *AtSMC1* and *AtSMC3* loci. Genomic maps showing the relative positions of *AtSMC1*, *PTPG* and *AtSMC3*, as well as cDNA fragments that were analyzed, are shown. The black boxes represent exons. Arrows (not drawn to scale) mark the position and orientation of primers used in this study. Broken arrows represent the main *AtSMC1* and *AtSMC3* transcriptional units. Bars separated by broken lines represent the cDNA fragment obtained from *AtSMC1*, *PTPG*, and an EST from GenBank. Bars, 0.4 kb.

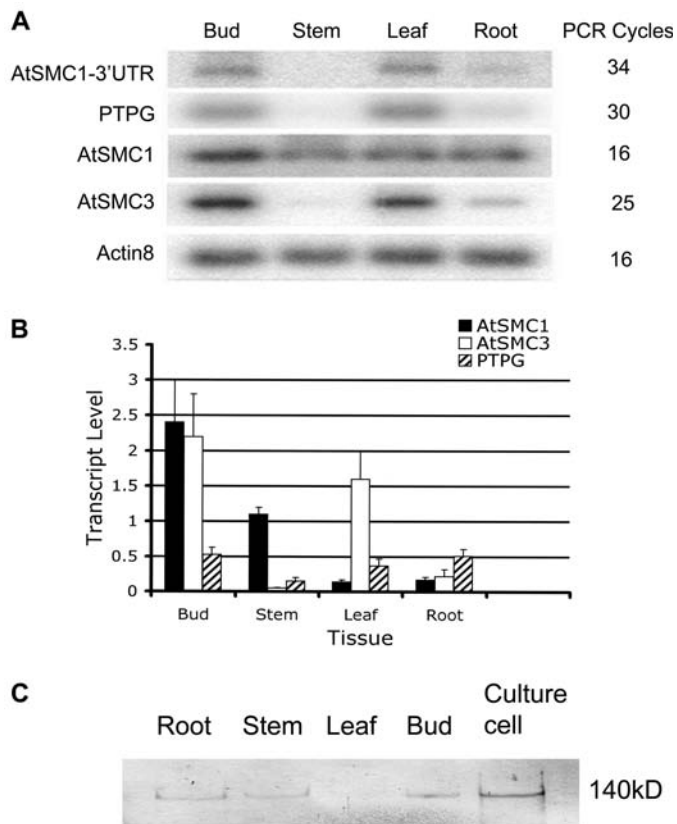


**Fig. 2.** AtSMC1 and AtSMC3 transcript and protein patterns differ in plant tissues. (A) *AtSMC1*, *AtSMC1-3'UTR*, *AtSMC3* and *PTPG* expression patterns were examined by RT-PCR analysis of oligo(dT)-generated total cDNA synthesized from RNA isolated from different plant organs: roots, stems, leaves, flower buds. Transcripts for *ACT8* were used as a control. RT-PCR products were analyzed by Southern blotting. The number of cycles used for PCR is shown to the right. (B) Relative levels of *AtSMC1*, *AtSMC3* and *PTPG* transcripts as determined by real-time PCR. Transcript levels were standardized relative to the level of *ACT8* cDNA in the sample. (C) AtSMC3 total protein (10 µg) from *Arabidopsis* root, stem, leaf, flower bud tissues and suspension culture cells was isolated and analyzed by western blotting using anti-AtSMC3 antibody.

### AtSMC3 exhibits novel localization patterns

Antibodies to AtSMC1 and AtSMC3 were generated in order to better study their distribution and subcellular localization in plants. The N-terminal halves of AtSMC1 and AtSMC3 were over expressed as His<sub>6</sub>-tagged proteins, purified from *E. coli* and used to raise antibody in rabbits. Although we were able to generate high quality antibody to AtSMC3, several attempts to produce a comparable AtSMC1 antibody were unsuccessful. While AtSMC1 antibodies did cross-react with *E. coli* produced antigen, they did not cross-react with an appropriate plant protein, either in western blots or immunolocalization experiments. Because the same region was used as the antigen for both proteins, it is not clear why difficulties with the AtSMC1 antibody were encountered.

The AtSMC3 antibody was found to be specific for AtSMC3; it did not cross-react with AtSMC1 proteins expressed in *E. coli*. In western blots, the antibody detected a

single 140 kDa protein in total protein extracts isolated from *Arabidopsis* roots, stems, leaves, flower buds and suspension cells (data not shown). AtSMC3 protein levels were similar in root, stem and flower bud tissues, but lower in leaf samples (Fig. 2B). The relatively high level of chloroplast proteins in this sample probably affects the relative, but not absolute amount of AtSMC3.

Because we were unsuccessful in raising antibody to AtSMC1 we are unable to directly compare the levels of the two proteins. However, the AtSMC3 western blot results indicate that the differences observed in transcript levels are not directly correlated with corresponding differences in protein levels. This suggests that *AtSMC3*, and possibly *AtSMC1*, may be regulated post-transcriptionally. However, further experiments are required to investigate this possibility.

Most immunolocalization studies in plants, including our report on the chromosomal localization of the meiotic cohesion protein SYN1, use 4% paraformaldehyde or Carnoy's solution for tissue fixation (Cai et al., 2003; Chen et al., 2002). When these fixation protocols were initially used to investigate the cellular localization of AtSMC3, labeling was observed in both the nucleus and cytoplasm (Fig. 3A, untreated cell). AtSMC3 labeling was generally not observed in the nucleolus, which also does not stain with DAPI. Control experiments with AtSMC3-depleted antibody or pre-immune serum were negative (data not shown), suggesting that AtSMC3 is present in both the nucleus and cytoplasm.

The subcellular localization of AtSMC3 was further investigated using a series of extractions on suspension culture cells. After digestion of the cell walls, soluble proteins were first extracted with salt (CSK buffer), and then detergent. While salt extraction of the cells reduced the cytoplasmic staining of AtSMC3, extraction with detergent eliminated most of the cytoplasmic labeling. The remaining AtSMC3 signal was found primarily inside the nucleus (Fig. 3A). When supernatant fractions containing proteins from the salt and detergent extractions were analyzed by western blotting, a strong AtSMC3 cross-reactive signal was observed in the detergent-extracted fraction with a considerably weaker signal from the salt extraction (Fig. 3B), consistent with the immunolocalization results. Subsequent treatment of the cells with DNase to remove DNA and chromatin-associated proteins eliminated the DAPI stained DNA but did not significantly affect the nuclear labeling of AtSMC3 (Fig. 3A). When the supernatant from DNase-treated cells was analyzed by western blotting, an AtSMC3 cross-reactive band was observed that was not observed in cells treated with no DNase, indicating that some chromatin-bound AtSMC3 was released by the DNase treatment (Fig. 3B). A considerably stronger signal was obtained from the pellet after DNase treatment, indicating that much of the nuclear AtSMC3 is bound to the nuclear matrix in the culture cells, which consist mainly of interphase cells. These results confirm that AtSMC3 is present in the cytoplasm of interphase cells and also demonstrate that a considerable portion of AtSMC3 is tightly associated with the nuclear matrix.

We next investigated the distribution of AtSMC3 in somatic and generative anther cells using immunolocalization. Studies in rat and human cells had previously shown that fixation with acetone or methanol:acetone resulted in strong nuclear SMC labeling and very little cytoplasmic staining (Eijpe et al., 2000;

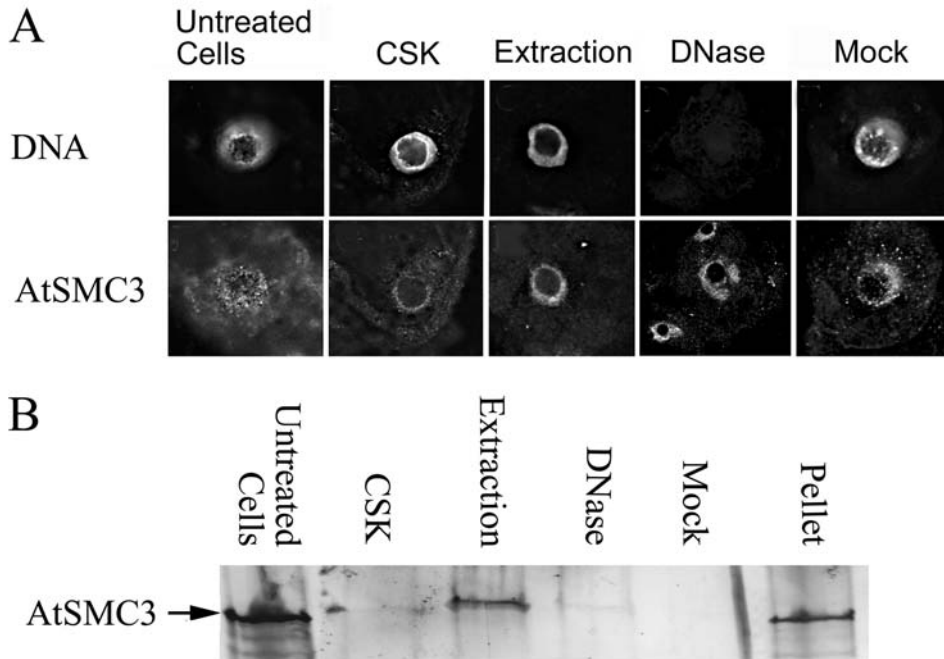


**Fig. 3.** AtSMC3 is present in the cytoplasm, nucleus and nuclear matrix of *Arabidopsis* suspension cells. (A) Images of anti-AtSMC3 labeling of interphase cells after various extractions and fixing with 4% paraformaldehyde. Cells were sequentially extracted with salt (CSK) followed by detergent extraction buffer to remove soluble cytoplasmic proteins, and subsequently treated with DNase. Untreated cells and buffer without DNase (mock) were used as controls. DNA was stained with DAPI. AtSMC3 was detected with anti-AtSMC3 antibody followed by treatment with Alexa Fluor 488-labeled secondary antibody. Scale bar: 10  $\mu$ m. (B) Western blot analysis of AtSMC3 eluted by the series of extractions as described for A. Proteins from these extractions were analyzed by western blotting with anti-AtSMC3 antibody. Cells before treatment were used as the control.

Gregson et al., 2001). Similar to the results obtained for animal cells, we found that methanol:acetone fixation of *Arabidopsis* cells reduced the cytoplasmic AtSMC3 signal and allowed us to better visualize AtSMC3 during mitosis and meiosis.

Strong chromosomal labeling with the anti-AtSMC3 antibody was observed in somatic cells from interphase to anaphase (Fig. 4). However, beginning at approximately metaphase, the antibody also appeared to co-localize with the mitotic spindle. In order to investigate this unexpected result further, triple labeling experiments were conducted with DAPI (blue), anti-AtSMC3 (red) antibody and anti- $\beta$ -tubulin (green) antibody. During interphase and early prophase, AtSMC3 labeling was confined to the nucleus with strong  $\beta$ -tubulin labeling around the outside of the nucleus (Fig. 4A). By metaphase AtSMC3 labeling of the chromosomes was reduced and much of the labeling was now found to overlap with the  $\beta$ -tubulin staining (Fig. 4B). During anaphase and telophase a strong AtSMC3 signal was associated with the microtubule spindle and there was weak labeling of the chromosomes (Fig. 4C,D). During cytokinesis AtSMC3 labeling was again found to associate with the chromatin (data not shown). Labeling patterns identical to those shown in Fig. 4A–D were also observed with *Arabidopsis* culture cells (data not shown) indicating that the localization pattern we observed was common to most somatic cells. Interestingly, in tapetal cells that were undergoing endoreduplication, AtSMC3 co-localized with both the chromosomes and phragmoplast-associated  $\beta$ -tubulin (Fig. 4E).

Immunofluorescent staining of AtSMC3 was also performed on wild-type microsporocytes to study the distribution of AtSMC3 during meiosis. Similar to the staining pattern observed for somatic cells, strong AtSMC3 staining was observed in the nucleus during meiotic interphase I, while the anti- $\beta$ -tubulin antibody stained the preprophase band around the outside of the nucleus (Fig. 5A). As cells progressed through leptotene, zygotene and pachytene AtSMC3 localized

with the condensing chromatin, while anti- $\beta$ -tubulin staining of the microtubules was observed throughout the cytoplasm (Fig. 5B). During diplotene, strong AtSMC3 staining of the condensing chromosomes was observed while the anti- $\beta$ -tubulin stained the extensive microtubule network (Fig. 5C). No AtSMC3 labeling of the cytoplasmic microtubule arrays was observed during interphase or prophase. By diakinesis the AtSMC3 signal became more diffuse and appeared to begin to separate from the chromosomes at the time depolymerization of the cytoplasmic microtubule network was observed (Fig. 5D). Similar to our observations for metaphase in somatic cells, AtSMC3 was found on both the chromosomes and spindle during meiotic metaphase I and anaphase I (Fig. 5E,F). During metaphase and anaphase the strongest chromosomal labeling appeared to coincide with the centromeres. By telophase I AtSMC3 was no longer detected on the chromosomes, but still showed strong co-localization with the  $\beta$ -tubulin signal (Fig. 5G). Weak centromeric labeling of AtSMC3 was again observed at metaphase II (data not shown). AtSMC3 was primarily detected on the spindle during anaphase II and observed throughout the cell at telophase II (Fig. 5H). Results similar to those shown in Fig. 5 were also obtained with paraformaldehyde-fixed cells by modifying the labeling and washing procedures, indicating that these results are not an artifact of the methanol-acetone fixation (data not shown). Therefore, AtSMC3 localizes to the chromosomes of meiotic prophase cells and primarily to the spindles during metaphase and anaphase of meiosis.

The images shown in Figs 4 and 5 represent relatively intact cells that maintain the cell structure. While this technique allows visualization of AtSMC3 on both the chromosomes and the spindle, it does not produce high-resolution images of the chromosomes. Therefore, we also analyzed AtSMC3 localization on chromosome spreads. The distribution of AtSMC3 on spreads of meiotic prophase chromosomes was very similar to those previously reported for SYN1 (Cai et al.,

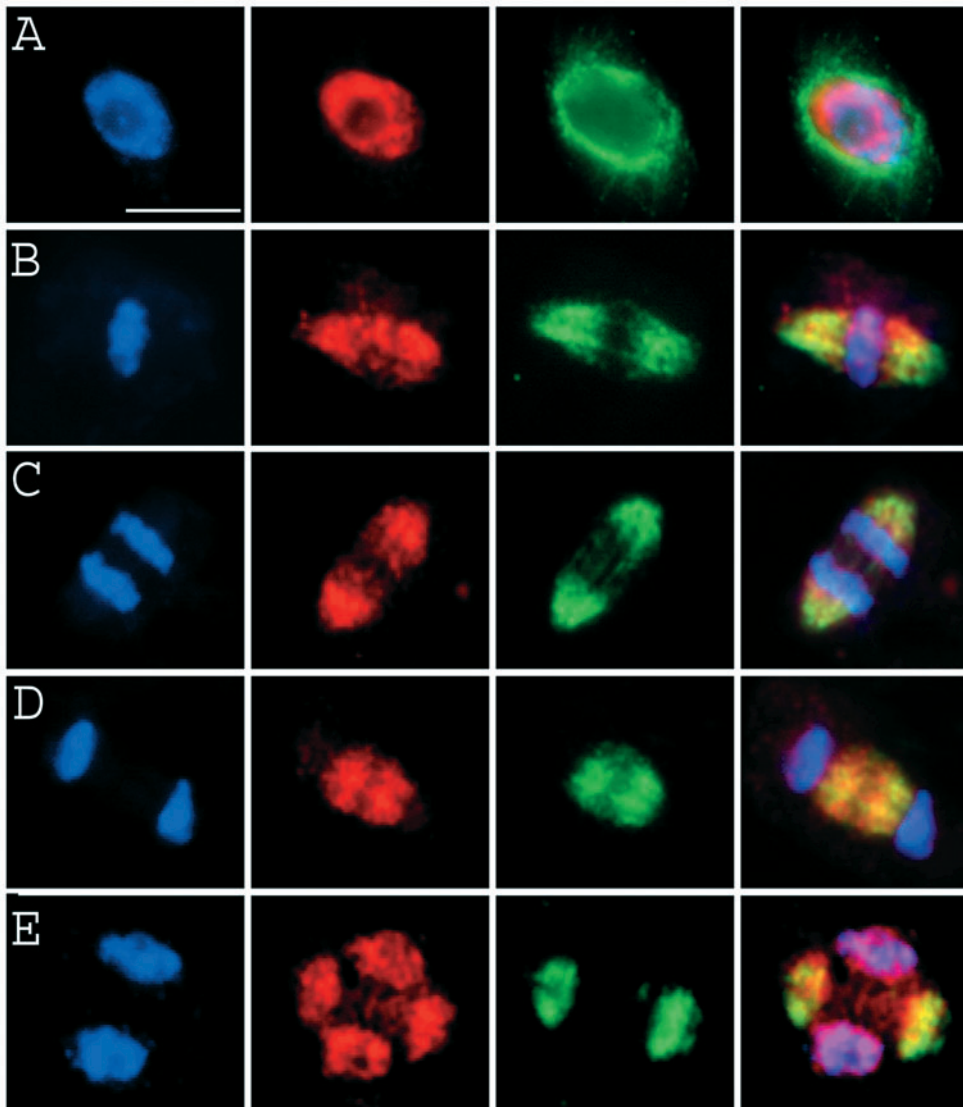


**Fig. 4.** AtSMC3 localizes to the chromosomes and spindles in *Arabidopsis* somatic cells. Fluorescence immunolocalization using anti-AtSMC3 antibody (red), anti- $\beta$ -tubulin antibody (green), DAPI stained DNA (blue), and the merged images (right column). (A) interphase; (B) metaphase; (C) anaphase; (D) telophase; (E) tapetal cell after nuclear division. Bar, 10  $\mu$ m.

2003). Specifically, AtSMC3 was found to localize along sister chromatids from leptotene to diakinesis. An example of the results obtained from the chromosome spreads is shown in Fig. 6A,B. Strong labeling of both AtSMC3 and SYN1 can be observed along the axial elements of sister chromatids as they pair during pachytene. This labeling pattern is consistent with the predicted role of the meiotic cohesin complex in synaptonemal complex formation (Eijpe et al., 2000).

#### SYN1 is required for the normal localization of AtSMC3 to meiotic chromosomes

Studies in yeast have provided a considerable amount of information on the structure of the cohesin complex and interactions between the SMC and non-SMC subunits (Haering et al., 2002; Haering et al., 2004). However, very little is known about how sister chromatid cohesion is established (Riedel et al., 2004). In particular, it is not clear if the SMC and non-SMC subunits bind chromosomes individually or if they must bind as a complex. In order to determine if SYN1 is required for the

loading of AtSMC3 onto meiotic chromosomes, we examined the distribution of AtSMC3 in microsporocytes of *syn1* homozygous mutant plants. In meocytes of *syn1* plants, AtSMC3 was observed normally in the nucleus during meiotic interphase (not shown). However, by early leptotene AtSMC3 labeling appeared weak and punctate (Fig. 7E) in contrast to the strong uniform labeling observed in wild-type meocytes (Fig. 7A). During zygotene and pachytene, chromosomal labeling of AtSMC3 became progressively weaker in the mutant. While some labeling along the sister chromatids was observed, many regions of the condensed chromosomes lacked visible AtSMC3 labeling (Fig. 7F,G). By diakinesis, AtSMC3 labeling of the chromosomes was much weaker; most of the signal was distributed throughout the cell (Fig. 7H). The remaining chromosomally localized AtSMC3 was typically observed as discrete spots that tended to correspond to the centromeres. Similar to our observations for cells at diakinesis, AtSMC3 labeling was typically observed at the centromeres of metaphase I cells (Fig. 7K). By late telophase II, AtSMC3

labeling was found throughout the cytoplasm (Fig. 7L) as it was in wild-type meiocytes (Fig. 5H).

The absence of SYN1 clearly affected the binding of

AtSMC3 to the chromosomes and resulted in increased cytoplasmic AtSMC3; it did not, however, appear to affect its subsequent relocalization to the spindle. Although *syn1* meiocytes show abnormalities in the microtubule spindle due to alterations in the distribution of chromosomes, AtSMC3 was consistently found to co-localize with the spindle during later stages of meiosis (Figs 7I-K). Therefore, while SYN1 is required for the proper loading of AtSMC3 onto chromosomes, it is not required for the re-localization of the protein to the meiotic spindle. Furthermore, although major alterations in the distribution of AtSMC3 are observed along the arms of meiotic chromosomes in the absence of SYN1, AtSMC3 was still found to associate with the centromeres.

### Discussion

SMC1 and SMC3 function as a heterodimer in the mitotic and meiotic cohesin complexes of many organisms. While it is clear that the proteins act as a complex to establish and maintain sister chromatid cohesion, differences in the distribution of different cohesin subunits have been identified in a number of organisms (Birkenbihl and Subramani, 1995; Eijpe et al., 2000; Eijpe et al., 2003; Gregson et al., 2001; Gregson et al., 2002). Likewise, there have been several reports suggesting that SMC1 and/or SMC3 have roles beyond sister chromatid cohesion in animal cells (Ghiselli et al., 1999; Gregson et al., 2001; Kim et al., 2002; Shimizu et al., 1998; Yazdi et al., 2002).

In this report we present the results of a detailed analysis of the expression and protein distribution patterns of *Arabidopsis* AtSMC3. We show that AtSMC3 is present in both the cytoplasm and nucleus of somatic and generative cells. In the nucleus it is present on chromosomes and in the nuclear matrix. During mitosis and meiosis AtSMC3 localizes with sister chromatids from prophase until late anaphase. Beginning at metaphase and extending through telophase it is primarily associated with the spindle. These results indicate that in addition to its conserved role in sister chromatid cohesion, AtSMC3 may also have a role in the spindle of plant cells.

Similar to our observations for AtSMC3, SMC1 was also found in the cytoplasm in humans and bound to the nuclear matrix in animal cells (Gregson et al., 2001). Human SMC3 has been shown to be part of the cohesin complex as well as the RC-1 complex, which is involved in DNA repair (Jessberger et al., 1993). However, at this time the role of SMC proteins in the nuclear matrix is not clear. It is possible that cohesin proteins in the nuclear matrix are involved in chromosome organization and the establishment of chromosome boundaries. It has also been suggested that nuclear-matrix-associated cohesin may be involved in the organization of the spindle during mitosis (Gregson et al., 2001). Based on results from our immunolocalization studies, discussed below, this may also be a possibility for AtSMC3.

The presence of cytoplasmic AtSMC3 could reflect a functional role of the protein in the cytoplasm, or merely

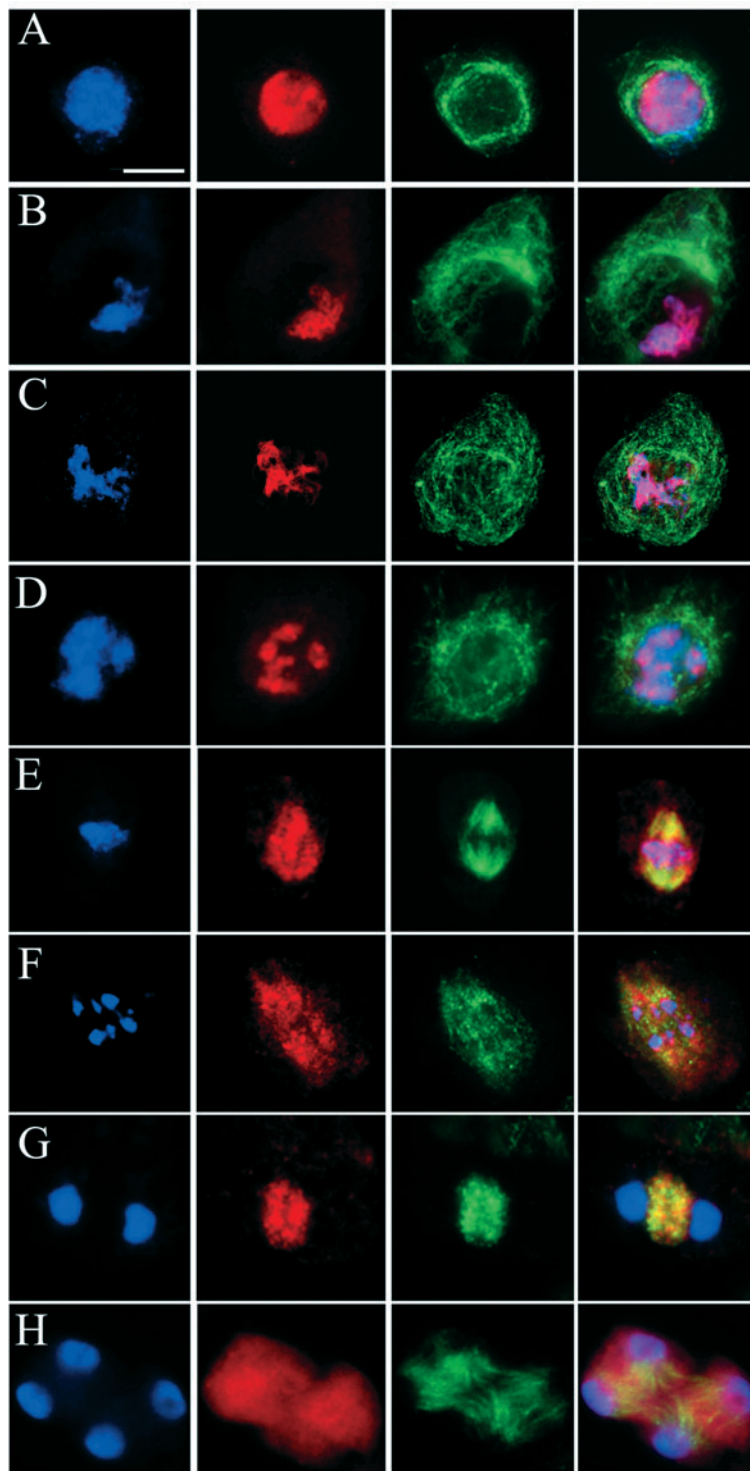


**Fig. 5.** AtSMC3 localizes to chromosomes and spindles in *Arabidopsis* meiocytes. Fluorescence immunolocalization using anti-AtSMC3 antibody (red), anti- $\beta$ -tubulin antibody (green), DNA stained with DAPI (blue), and the merged images (right column). (A) Interphase; (B) pachytene; (C) diplotene; (D) diakinesis; (E) metaphase I; (F) anaphase I; (G) telophase I; (H) telophase II. Bar, 10  $\mu$ m.

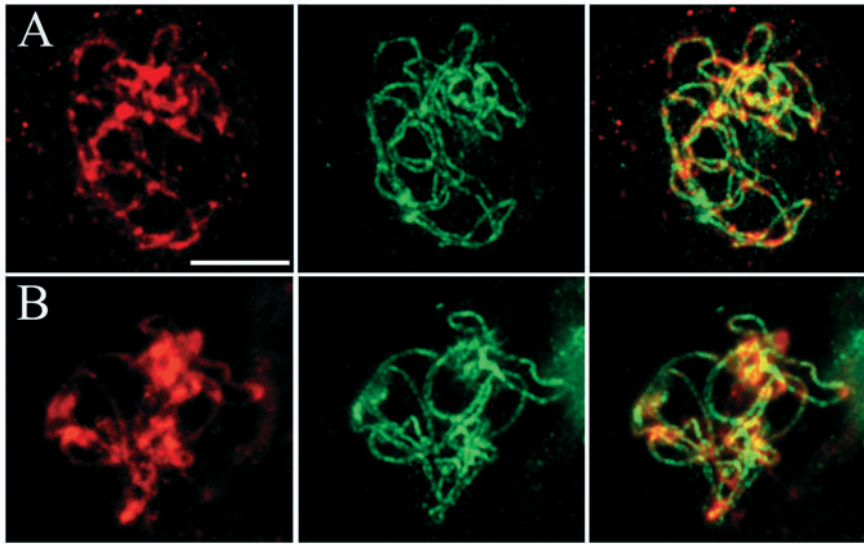


**Fig. 6.** AtSMC3 and SYN1 localize to axial elements of pachytene chromosomes. Immunolocalization of AtSMC3 (A, green) and SYN1 (B, green) on meiotic spreads of pachytene chromosomes. DNA was counterstained with DAPI (red). The merged images are shown on the right. Bar, 10  $\mu$ m.

the fact that the cytoplasm represents a storage site for the protein between cell divisions. An extracellular form of SMC3 has been identified as the murine Bamacan gene, which encodes a high density chondroitin sulfate proteoglycan present in basement membranes (Ghiselli et al., 1999). Bamacan proteoglycan has been shown to be a normal constituent of the basement membranes of several animal tissues (McCarthy et al., 1989); however, the exact function of the Bamacan protein has yet to be determined.

Because we were unable to raise antibody to AtSMC1, we were unable to determine at this time if it is also present in the cytoplasm or bound to the nuclear matrix in plant cells. However, cytoplasmic staining of paraformaldehyde-fixed cells is not normally observed with antibodies to SYN1 (Cai et al., 2003), SYN2, SYN3 or SYN4 (our unpublished data). Therefore, not all components of the *Arabidopsis* cohesin complex are present at high levels in the cytoplasm. This may

be a reflection of the fact that the klesins (SCC1/REC8) represent the regulatory subunit of the complex and undergo proteolysis during cohesion release. Therefore, they are not recycled between nuclear divisions as is expected for the SMC proteins (Rao et al., 2001).

During mitotic and meiotic interphase and prophase AtSMC3 associates with the chromosomes. However, beginning at approximately metaphase, AtSMC3 co-localizes with both the chromosomes and the microtubule spindle. By anaphase chromosomal AtSMC3 labeling is confined primarily to the centromeres, while co-localization with the microtubules is observed until cytokinesis. Although the correlation between the AtSMC3 and  $\beta$ -tubulin labeling was quite strong, the anti-AtSMC3 labeling pattern was more diffuse than the  $\beta$ -tubulin labeling and did not show distinct labeling of the spindle fibers (Figs 3 and 4). This suggests that AtSMC3 may not be directly associated with the microtubules, but rather one or more

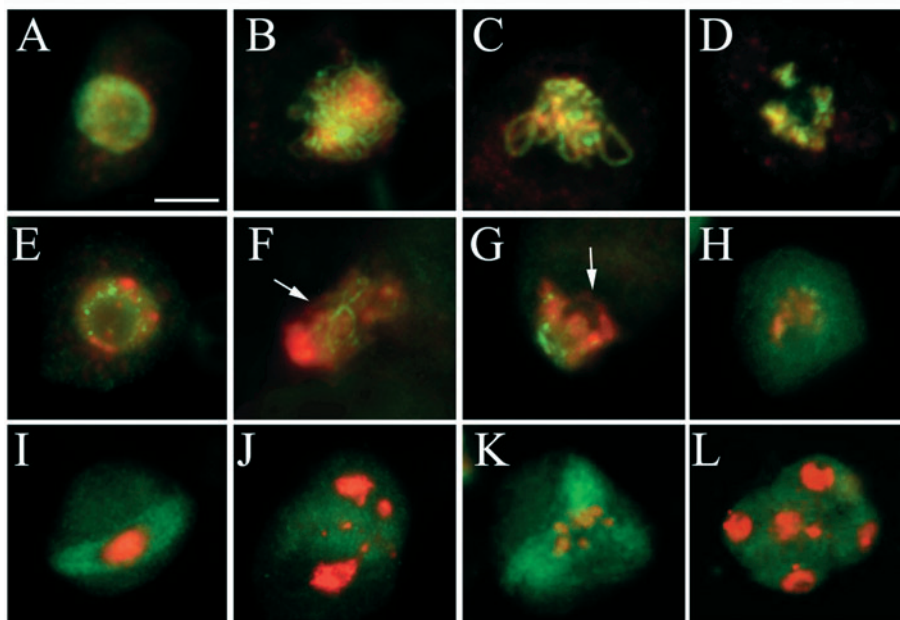


**Fig. 7.** SYN1 is required for proper localization of AtSMC3. Immunolocalization of AtSMC3 (green) in meiocytes of wild-type (A-D) and *syn1* (E-L) plants. DNA was counter-stained with DAPI (red). (A,E) interphase; (B,F) zygotene; (C,G) pachytene; (D,H) diakinesis; (I) metaphase I; (J) telophase I; (K) anaphase II; (L) telophase II. Arrows indicate chromosome regions not labeled with anti-AtSMC3 antibody. Bar, 10  $\mu$ m.

spindle-associated proteins. Our results represent the first report of a cohesin protein actually associating with the mitotic and meiotic spindles. SMC1, SMC3 and SA1 have been found at the mitotic spindle pole during late metaphase and early anaphase in HeLa cells (Gregson et al., 2001). However, unlike AtSMC3, the proteins are not observed along the spindle.

At this time the role of AtSMC3 in spindle structure/function is unknown. It is possible that it functions in spindle assembly and/or association of the chromosomes with the spindle. It has been suggested that animal cohesins may play a role in either the assembly and/or maintenance of the spindles (Gregson et al., 2001; Shimizu et al., 1998). Consistent with this theory, hSMC3 has been shown to interact with the kinesin superfamily proteins KIF3A and KIF3B and the kinesin superfamily-associated protein SMAP (Shimizu et al., 1998). It is possible that AtSMC3 plays a similar role. However, our failure to detect SYN1 (Cai et al., 2003), SYN2, SYN3 and SYN4 (our unpublished data) at the spindles indicates that AtSMC3 is not functioning as part of the cohesin complex at the spindle.

While further experiments are required to determine the exact nature of the AtSMC3-spindle interaction and the role of AtSMC3 in the spindle, several factors indicate that the labeling patterns we observed are specific for AtSMC3. (1) The anti-AtSMC3 antibody identified one distinct protein of the proper molecular mass in western blots. (2) Identical labeling patterns were observed for AtSMC3 and the meiotic cohesin protein, SYN1 on spreads of meiotic chromosomes. (3) Although fractionation studies showed that AtSMC3 is present in the cytoplasm of interphase cells, the anti-AtSMC3 antibody did not label the microtubule arrays in these cells. Therefore, the labeling is not due to the non-specific interaction of the antibody with microtubules.

Considerable information is available on the structure of the cohesin complex (Haering et al., 2002; Haering et al., 2004). However, very little is known about how sister chromatid cohesion is established, including if the SMC and non-SMC subunits bind chromosomes individually or as a complex. Our analysis of AtSMC3 distribution in the *syn1* mutant indicates that SYN1 is required for the proper binding of SMC3 to chromosomes. While SMC3 is able to bind to chromosomes in the absence of SYN1, its distribution is markedly altered beginning at early leptotene (Fig. 7). In wild-type meiocytes strong anti-AtSMC3 labeling is found along the lateral and axial elements during prophase. In contrast, in meiocytes of *syn1* plants AtSMC3 labeling of the chromosomes was considerably weaker and more punctate in appearance; labeling of lateral elements was not observed. Therefore, while AtSMC3 and presumably the rest of the cohesin complex can bind chromosomes in the absence of SYN1, the complex does not bind normally. Our current results do not indicate if SYN1 is required for the initial binding of SMC3 to the chromosomes or only to maintain its binding. However, based on AtSMC3 labeling patterns during early prophase, we suggest that SYN1 is actually required for proper binding of the complex.

Results from numerous studies in a range of organisms has lead to the widely accepted model that cohesin proteins load as a complex to establish meiotic sister chromatid cohesion during DNA replication (Uhlmann and Nasmyth, 1998). While DNA binding studies have shown that SMC proteins can directly bind to DNA (Akhmedov et al., 1998; Akhmedov et

al., 1999; Chiu et al., 2004), similar studies have not been performed for the klesin subunits. Therefore, it is generally thought that the SMC proteins are responsible for cohesin complex binding to the chromosomes. Our results and those from other studies raise the interesting possibility that the klesin subunits may play an important role in cohesin complex binding. Localization of several cohesin subunits during rat meiosis showed that REC8 appeared in the nucleus shortly before premeiotic S-phase and formed axial element-like structures beginning at premeiotic S phase (Eijpe et al., 2003). Subsequently SMC1 $\beta$  and SMC3 were detected on the chromosomes. Furthermore, while essentially no binding of SMC1 was observed to chromosome spreads in the absence of SCC1, low levels of SCC1 were observed in the absence of SMC1 in yeast cells (Weitzer et al., 2003). Further experiments are clearly required to determine how cohesin complexes are loaded on chromosomes and to investigate the possibility that the klesin subunit plays an important role in the initial binding of the complex. However, these studies suggest that in addition to their gatekeeper role in the cohesin complex, klesin subunits may also directly participate in the binding of the complex to the chromosomes.

This research was supported by grants from the US Department of Agriculture (grant no. 00-35301-9341) and the National Science Foundation (grant no. MCB-0322171). The Ohio Board of Regents and Miami University also contributed funds to purchase the microscopes used in this work. The E7 anti- $\beta$ -tubulin antibody developed by M. Klymkowsky was obtained from the Developmental Studies Hybridoma Bank developed under the auspices of the NICHD. We are grateful to Jonathon Jones for the *Arabidopsis* cell cultures, and Roy Brown, Meghan Holdorf and Yumin Chen for helpful discussions and comments on the manuscript.

## References

- Akhmedov, A. T., Frei, C., Tsai-Pflugfelder, M., Kemper, B., Gasser, S. M. and Jessberger, R. (1998). Structural maintenance of chromosomes protein C-terminal domains bind preferentially to DNA with secondary structure. *J. Biol. Chem.* **273**, 24088-24094.
- Akhmedov, A. T., Gross, B. and Jessberger, R. (1999). Mammalian SMC3 C-terminal and coiled-coil protein domains specifically bind palindromic DNA, do not block DNA ends, and prevent DNA bending. *J. Biol. Chem.* **274**, 38216-38224.
- An, Y. Q., McDowell, J. M., Huang, S., McKinney, E. C., Chambliss, S. and Meagher, R. B. (1996). Strong, constitutive expression of the *Arabidopsis* ACT2/ACT8 actin subclass in vegetative tissues. *Plant J.* **10**, 107-121.
- Bai, X., Peirson, B. N., Dong, F., Xue, C. and Makaroff, C. A. (1999). Isolation and characterization of *SYN1*, a *RAD21*-like gene essential for meiosis in *Arabidopsis*. *Plant Cell* **11**, 417-430.
- Berger, B., Wilson, D. B., Wolf, E., Tonchev, T., Milla, M. and Kim, P. S. (1995). Predicting coiled coils by use of pairwise residue correlations. *Proc. Natl. Acad. Sci. USA* **92**, 8259-8263.
- Bhatt, A. M., Lister, C., Page, T., Fransz, P., Findlay, K., Jones, G. H., Dickinson, H. G. and Dean, C. (1999). The *DIF1* gene of *Arabidopsis* is required for meiotic chromosome segregation and belongs to the *REC8/RAD21* cohesin gene family. *Plant J.* **19**, 463-472.
- Birkenbihl, R. P. and Subramani, S. (1995). The *rad21* gene product of *Schizosaccharomyces pombe* is a nuclear, cell cycle-regulated phosphoprotein. *J. Biol. Chem.* **270**, 7703-7711.
- Buonomo, S. B., Clyne, R. K., Fuchs, J., Loidl, J., Uhlmann, F. and Nasmyth, K. (2000). Disjunction of homologous chromosomes in meiosis I depends on proteolytic cleavage of the meiotic cohesin Rec8 by separin. *Cell* **103**, 387-398.
- Cai, X., Dong, F., Edelman, R. E. and Makaroff, C. A. (2003). The *Arabidopsis* SYN1 cohesin protein is required for sister chromatid arm cohesion and homologous chromosome pairing. *J. Cell Sci.* **116**, 2999-3007.

- Chen, C., Marcus, A., Li, W., Hu, Y., Calzada, J. P., Grossniklaus, U., Cyr, R. J. and Ma, H. (2002). The *Arabidopsis* *ATK1* gene is required for spindle morphogenesis in male meiosis. *Development* **129**, 2401-2409.
- Chiu, A., Revenkova, E. and Jessberger, R. (2004). DNA interaction and dimerization of eukaryotic SMC hinge domains. *J. Biol. Chem.* **279**, 26233-26242.
- Cobbe, N. and Heck, M. M. (2000). Review: SMCs in the world of chromosome biology – from prokaryotes to higher eukaryotes. *J. Struct. Biol.* **129**, 123-143.
- Dong, F., Cai, X. and Makaroff, C. A. (2001). Cloning and characterization of two *Arabidopsis* genes that belong to the *RAD21/REC8* family of chromosome cohesin proteins. *Gene* **271**, 99-108.
- Eijpe, M., Heyting, C., Gross, B. and Jessberger, R. (2000). Association of mammalian SMC1 and SMC3 proteins with meiotic chromosomes and synaptonemal complexes. *J. Cell Sci.* **113**, 673-682.
- Eijpe, M., Offenberger, H., Jessberger, R., Revenkova, E. and Heyting, C. (2003). Meiotic cohesin REC8 marks the axial elements of rat synaptonemal complexes before cohesins SMC1beta and SMC3. *J. Cell Biol.* **160**, 657-670.
- Fousteri, M. I. and Lehmann, A. R. (2000). A novel SMC protein complex in *Schizosaccharomyces pombe* contains the Rad18 DNA repair protein. *EMBO J.* **19**, 1691-1702.
- Ghiselli, G., Siracusa, L. D. and Iozzo, R. V. (1999). Complete cDNA cloning, genomic organization, chromosomal assignment, functional characterization of the promoter, and expression of the murine *Bamacan* gene. *J. Biol. Chem.* **274**, 17384-17393.
- Gregson, H. C., Schmiesing, J. A., Kim, J. S., Kobayashi, T., Zhou, S. and Yokomori, K. (2001). A potential role for human cohesin in mitotic spindle aster assembly. *J. Biol. Chem.* **276**, 47575-47582.
- Gregson, H. C., van Hooser, A. A., Ball, A. R., Jr, Brinkley, B. R. and Yokomori, K. (2002). Localization of human SMC1 protein at kinetochores. *Chromosome Res.* **10**, 267-277.
- Gruber, S., Haering, C. H. and Nasmyth, K. (2003). Chromosomal cohesin forms a ring. *Cell* **112**, 765-777.
- Haering, C. H., Lowe, J., Hochwagen, A. and Nasmyth, K. (2002). Molecular architecture of SMC proteins and the yeast cohesin complex. *Mol. Cell* **9**, 773-788.
- Haering, C. H., Schoffnegger, D., Nishino, T., Helmhart, W., Nasmyth, K. and Lowe, J. (2004). Structure and stability of cohesin's Smc1-kleisin interaction. *Mol. Cell* **15**, 951-964.
- Hagstrom, K. A., Holmes, V. F., Cozzarelli, N. R. and Meyer, B. J. (2002). *C. elegans* condensin promotes mitotic chromosome architecture, centromere organization, and sister chromatid segregation during mitosis and meiosis. *Genes Dev.* **16**, 729-742.
- Harlow, E. and Lane, D. (1999). *Using antibodies: A laboratory manual*. Cold Spring Harbor, N.Y.: Cold Spring Harbor Laboratory.
- Hauf, S., Waizenegger, I. C. and Peters, J. M. (2001). Cohesin cleavage by separase required for anaphase and cytokinesis in human cells. *Science* **293**, 1320-1323.
- Hirano, T. (2002). The ABCs of SMC proteins: two-armed ATPases for chromosome condensation, cohesion, and repair. *Genes Dev.* **16**, 399-414.
- Jessberger, R. (2002). The many functions of SMC proteins in chromosome dynamics. *Nat. Rev. Mol. Cell Biol.* **3**, 767-778.
- Jessberger, R., Podust, V., Hubscher, U. and Berg, P. (1993). A mammalian protein complex that repairs double-strand breaks and deletions by recombination. *J. Biol. Chem.* **268**, 15070-15079.
- Kim, S., Xu, B. and Kastan, M. (2002). Involvement of the cohesin protein, Smc1, in Atm-dependent and independent responses to DNA damage. *Genes Dev.* **16**, 560-570.
- Klein, F. M. P., Galova, M., Buonomo, S. B., Michaelis, C., Nairz, K. and Nasmyth, K. (1999). A central role for cohesins in sister chromatid cohesion, formation of axial elements, and recombination during yeast meiosis. *Cell* **98**, 91-103.
- Lin, Y., Larson, K. L., Dorer, R. and Smith, G. R. (1992). Meiotically induced *rec7* and *rec8* genes of *Schizosaccharomyces pombe*. *Genetics* **132**, 75-85.
- Liu, C. M. and Meinke, D. W. (1998). The titan mutants of *Arabidopsis* are disrupted in mitosis and cell cycle control during seed development. *Plant J.* **16**, 21-31.
- Liu, C. M., McElver, J., Tzafir, I., Joosen, R., Wittich, P., Patton, D., van Lammeren, A. A. and Meinke, D. (2002). Condensin and cohesin knockouts in *Arabidopsis* exhibit a titan seed phenotype. *Plant J.* **29**, 405-415.
- Losada, A., Hirano, M. and Hirano, T. (1998). Identification of *Xenopus* SMC protein complexes required for sister chromatid cohesion. *Genes Dev.* **12**, 1986-1997.
- Losada, A., Yokochi, T., Kobayashi, R. and Hirano, T. (2000). Identification and characterization of SA/Sec3p subunits in the *Xenopus* and human cohesin complexes. *J. Cell Biol.* **150**, 405-416.
- Losada, A., Hirano, M. and Hirano, T. (2002). Cohesin release is required for sister chromatid resolution, but not for condensin-mediated compaction, at the onset of mitosis. *Genes Dev.* **16**, 3004-3016.
- McCarthy, K., Accavitti, M. and Couchman, J. (1989). Immunological characterization of a basement membrane-specific chondroitin sulfate proteoglycan. *J. Cell Biol.* **109**, 3187-3198.
- Michaelis, C., Ciosk, R. and Nasmyth, K. (1997). Cohesins: chromosomal proteins that prevent premature separation of sister chromatids. *Cell* **91**, 35-45.
- Ono, T., Losada, A., Hirano, M., Myers, M. P., Neuwald, A. F. and Hirano, T. (2003). Differential contributions of condensin I and condensin II to mitotic chromosome architecture in vertebrate cells. *Cell* **115**, 109-121.
- Peirson, B. N., Bowling, S. E. and Makaroff, C. A. (1997). A defect in synapsis causes male sterility in a T-DNA-tagged *Arabidopsis thaliana* mutant. *Plant J.* **11**, 659-669.
- Prieto, I. S. J. A., Pezzi, N., Kremer, L., Martinez-A, C., Rufas, J. S. and Barbero, J. L. (2001). Mammalian STAG3 is a cohesin specific to sister chromatid arms in meiosis I. *Nat. Cell Biol.* **3**, 761-776.
- Rao, H., Uhlmann, F., Nasmyth, K. and Varshavsky, A. (2001). Degradation of a cohesin subunit by the N-end rule pathway is essential for chromosome stability. *Nature* **410**, 955-959.
- Revenkova, E., Eijpe, M., Heyting, C., Gross, B. and Jessberger, R. (2001). A novel meiosis-specific isoform of mammalian SMC1. *Mol. Cell Biol.* **21**, 6984-6998.
- Revenkova, E., Eijpe, M., Heyting, C., Hodges, C. A., Hunt, P. A., Liebe, B., Scherthan, H. and Jessberger, R. (2004). Cohesin SMC1 beta is required for meiotic chromosome dynamics, sister chromatid cohesion and DNA recombination. *Nat. Cell Biol.* **6**, 555-562.
- Riedel, C. G., Gregan, J., Gruber, S. and Nasmyth, K. (2004). Is chromatin remodeling required to build sister-chromatid cohesion? *Trends Biochem. Sci.* **29**, 389-392.
- Schmiesing, J. A., Gregson, H. C., Zhou, S. and Yokomori, K. (2000). A human condensin complex containing hCAP-C-hCAP-E and CNAP1, a homolog of *Xenopus* XCAP-D2, colocalizes with phosphorylated histone H3 during the early stage of mitotic chromosome condensation. *Mol. Cell Biol.* **20**, 6996-7006.
- Shimizu, K., Shirataki, H., Honda, T., Minami, S. and Takai, Y. (1998). Complex formation of SMAP/KAP3, a KIF3A/B ATPase motor-associated protein, with a human chromosome-associated polypeptide. *J. Biol. Chem.* **273**, 6591-6594.
- Siddiqui, N. U., Stronghill, P. E., Dengler, R. E., Hasenkampf, C. A. and Riggs, C. D. (2003). Mutations in *Arabidopsis* condensin genes disrupt embryogenesis, meristem organization and segregation of homologous chromosomes during meiosis. *Development* **130**, 3283-3295.
- Soppa, J. (2001). Prokaryotic structural maintenance of chromosomes (SMC) proteins: distribution, phylogeny, and comparison with MukBs and additional prokaryotic and eukaryotic coiled-coil proteins. *Gene* **278**, 253-264.
- Strunnikov, A. V., Larionov, V. L. and Koshland, D. (1993). *SMC1*: an essential yeast gene encoding a putative head-rod-tail protein is required for nuclear division and defines a new ubiquitous protein family. *J. Cell Biol.* **123**, 1635-1648.
- Sumara, I., Vorlaufer, E., Stukenberg, P. T., Kelm, O., Redemann, N., Nigg, E. A. and Peters, J. M. (2002). The dissociation of cohesin from chromosomes in prophase is regulated by Polo-like kinase. *Mol. Cell* **9**, 515-525.
- Tanaka, T., Cosma, M. P., Wirth, K. and Nasmyth, K. (1999). Identification of cohesin association sites at centromeres and along chromosome arms. *Cell* **98**, 847-858.
- Taylor, E. M., Moghraby, J. S., Lees, J. H., Smit, B., Moens, P. B. and Lehmann, A. R. (2001). Characterization of a novel human SMC heterodimer homologous to the *Schizosaccharomyces pombe* Rad18/Spr18 complex. *Mol. Biol. Cell* **12**, 1583-1594.
- Uhlmann, F. and Nasmyth, K. (1998). Cohesion between sister chromatids must be established during DNA replication. *Curr. Biol.* **8**, 1095-1101.
- Uhlmann, F., Lottspeich, F. and Nasmyth, K. (1999). Sister-chromatid separation at anaphase onset is promoted by cleavage of the cohesin subunit Scc1. *Nature* **400**, 37-42.
- Uhlmann, F., Wernic, D., Poupard, M. A., Koonin, E. V. and Nasmyth, K. (2000). Cleavage of cohesin by the CD clan protease separin triggers anaphase in yeast. *Cell* **103**, 375-386.

**Waizenegger, I. C., Hauf, S., Meinke, A. and Peters, J. M.** (2000). Two distinct pathways remove mammalian cohesin from chromosome arms in prophase and from centromeres in anaphase. *Cell* **103**, 399-410.

**Weitzer, S., Lehane, C. and Uhlmann, F.** (2003). A model for ATP hydrolysis-dependent binding of cohesin to DNA. *Curr. Biol.* **13**, 1930-1940.

**Yazdi, P., Wang, Y., Zhao, S., Patel, N., Lee, E. and Qin, J.** (2002). SMC1 is a downstream effector in the ATM/NBS1 branch of the human S-phase checkpoint. *Genes Dev.* **16**, 571-582.

**Yokobayashi, S., Yamamoto, M. and Watanabe, Y.** (2003). Cohesins determine the attachment manner of kinetochores to spindle microtubules at meiosis I in fission yeast. *Mol. Cell. Biol.* **23**, 3965-3973.